Ectopic and reentrant activation patterns in the posterior left atrium during stretch-related atrial fibrillation

Masatoshi Yamazaki[a,1], **David Filgueiras-Rama**[a,1], **Omer Berenfeld**[a,b,*], and **Jérôme Kalifa**[a]

[a]Center for Arrhythmia Research, Department of Internal Medicine, University of Michigan, Ann Arbor, MI, USA

[b]Department of Biomedical Engineering, University of Michigan, Ann Arbor, MI, USA

Abstract

Atrial fibrillation (AF) is the most common sustained cardiac arrhythmia in humans and is predicted to dramatically increase its prevalence in the future. There is experimental evidence that increasing stretch increases the dominance of the pulmonary veins (PVs) during AF in isolated hearts and ectopic activity in the isolated PVs, but the ionic mechanisms underlying such effects are not clear and the ability of the PVs to favorably host functional reentry during stretch cannot be excluded. We used a combination of endocardial–epicardial optical mapping with phase and spectral analysis to study stretch-related AF (SRAF) in normal isolated sheep hearts. We have found rapid AF sources in the posterior left atrium (PLA) and PV region and their activation frequency and level of organization correlated with intra-atrial pressure. Analysis of the surfaces' optical mapping data in the phase domain reveals that activation of the PLA consisted of alternating patterns of breakthroughs, reentries and relatively simple waves swiping across the mapped field. The patterns on the endocardial and epicardial PLA surface at any given moment of time of the SRAF could be either identical or not identical, and the activity in the thickness of the PLA wall is hypothesized to conform to either ectopic discharge or scroll waves, but a definite evidence for the presence of such mechanisms is currently lacking. Thus the understanding of the manner by which the mechano-electric feedback effects in the PLA, including the PVs, become important in the initiation and maintenance of AF requires further detailed investigation.

Keywords

Atrial fibrillation; Atrial dilatation; Optical mapping; Reentry; Ectopic activity; Pulmonary veins

1. Introduction

Atrial fibrillation (AF) is to date the most common sustained cardiac arrhythmia in humans and is predicted to dramatically increase its prevalence in the near future (Chen and Shen,

[*]Corresponding author. Center for Arrhythmia Research, Department of Internal Medicine, University of Michigan, 2800 Plymouth Road, Ann Arbor, MI 48109, USA. Tel.: +1 734 998 7560; fax: +1 734 998 7711., oberen@umich.edu (O. Berenfeld).
[1]Contributed equally.

Editors' note

Please see also related communications in this issue by Quinn and Kohl (2012) and Werdich et al. (2012).

2007). Antiarrhythmic drugs are only partially effective in treating AF, and have the potential for serious side effects, including life-threatening pro-arrhythmia. The pulmonary veins (PVs) and the anatomical region surrounding their antrum into the left atrium were found to play an important role in the initiation and maintenance of the arrhythmia. High-resolution mapping data and Fourier power spectrum analysis with its dominant frequency (DF) recently published by our group support the hypothesis that acute AF in the structurally normal sheep heart (Skanes et al., 1998; Berenfeld et al., 2000, 2002; Chen et al., 2000; Mandapati et al., 2000; Mansour et al., 2001) and in some patients (Sanders et al., 2005) is not a totally random phenomenon. These data are consistent with the widely accepted notion that paroxysmal AF in patients is initiated by focal triggers localized in one or more PVs (Haissaguerre et al., 1998) and is accessible to catheter-based ablation procedures (Haissaguerre et al., 2000b). On the other hand, in persistent AF the prevailing theory is that multiple random wavelets of activation coexist to create a chaotic cardiac rhythm, (Moe and Abildskov, 1959) and that AF ablative therapy is more challenging (Haissaguerre et al., 2000a; Benussi et al., 2000; Knight et al., 1997; Oral et al., 2006).

1.1. The structure and function of the pulmonary veins

There is experimental evidence that stretch increases the PVs to left atrium (LA) wave propagation and DF gradient during AF, (Mandapati et al., 2000; Kalifa et al., 2003) and ectopic activity in the isolated PVs, (Chang et al., 2007) thus pointing to an increase in the dominance of the PVs in AF maintenance, but the ionic mechanisms underlying such effect are not clear and the ability of the PVs to favorably host functional reentry during stretch cannot be excluded (Mandapati et al., 2000; Kalifa et al., 2003). The PVs are composed of a variety of tissues, including cardiomyocyte sleeves along with an outermost covering connective tissue that surrounds the veins (tunica adventitia), a middle layer (media) and an innermost layer (intima). In humans, myocardial continuity from the LA wall extending to the outer surface of the pulmonary venous walls is well recognized (de Bakker et al., 2002). In guinea pigs the middle layer of the PV is made up of cardiac muscle at the proximal end joining the atria and smooth muscle at the distal intra-pulmonary end (Cheung, 1981a). At the atrial muscle–smooth muscle junction located about 4 mm intrapulmonarily, there is a drastic reduction in vessel diameter from more than 0.8 mm at the cardiac portion to about 0.4 mm at the smooth muscle portion. Brunton and Fayrer (1876) first reported in 1876 that independent pulsation of the PV, suggestive of electrical activity, occurred in cats and rabbits even after activity of the heart had ceased. In isolated preparations of the PVs and the adjacent atrial tissue from guinea pigs, Cheung (1981a,b) showed in 1981 heterogeneous electro-physiology with different resting membrane potentials, responses to stimuli and automaticity between these two regions. Spontaneous pulsative beating of the atrial PV originating at the distal end of the PV and synchronous with atrial contraction was observed when a guinea pig thoracic wall was opened up and when the lungs were removed together with the heart for experimentation (Cheung, 1981a). The frequency of the spontaneous activity was variable but was usually maintained at about 0.5 Hz, which is significantly lower than the normal heart rate of that species at 230–380 beats/min (about 3.8–4.7 Hz). Chen et al. (2000) studied isolated canine and rabbit PVs and found rapid and low amplitude spiking activity of unknown mechanism in tissue beyond the end of the cardiomyocyte sleeve. In a subsequent study Chen et al. (2001) showed that cardiomyocytes isolated from

normal canine and rabbit PV can manifest automaticity, as well as after-depolarizations, which are enhanced by recognized atrial profibrillatory maneuvers such as chronic atrial tachypacing and in-vitro exposure to thyroid hormone by unknown mechanisms (Cha et al., 2005; Chen et al., 2002). Miyauchi et al. (2005) showed that heterogeneous PV repolarization properties are associated with the propensity to early after-depolarizations and triggered activity induced by isoproteranol and rapid pacing. These observations add to the possible mechanisms rendering the PVs vulnerable for arrhythmogenesis, such as marked tissue anisotropy, (Hocini et al., 2002) Ca^{2+}-handling (Honjo et al., 2003; Patterson et al., 2006) and arrhythmogenic response to local autonomic activity (Patterson et al., 2005). Indeed, compared with LA myocytes, PV sleeve cardiomyocytes display distinct electrophysiological properties in several ionic currents (Ehrlich et al., 2003) and several potassium channels distribution (Melnyk et al., 2005). Seol et al. (2008) characterized stretch activated currents in cardiomyocytes isolated from rabbit PVs and found distinct currents induced by swelling versus axial mechanical stretching of the myocytes. Both types of stretching induced anionic and nonselective cationic and currents obeying a positive monotonic *I–V* relationship, although the cationic currents activated faster than the anionic currents and were likely mediated through different channels (Seol et al., 2008).

1.2. Ectopic versus reentrant activity in the PVs

In the single cardiomyocytes isolated from the PVs of rabbits and studied by Seol et al. (2008) it is not clear whether the dominance of the PVs in the initiation and maintenance of AF depends on spatial heterogeneity in the distribution of currents, or alternatively in the relative increase in stretch due to the relative thinner myocardial wall in the PV sleeve compared with the walls of the atria (Nathan and Eliakim, 1966; Seol et al., 2008). The high propensity of normal PVs to generate ectopic activities raises an important question. Why paroxysmal AF is not even more common in the general population? Likely, additional pathophysiological factors are required to facilitate fibrillation maintenance by reentrant activities and/or spontaneous focal discharges (Nattel, 2005).

The notion that a localized source of reentrant activity could maintain AF was first postulated by Lewis (1925) in the early part of the twentieth century and subsequently by Scherf (1947). Many years later, Morillo et al. (1995) targeted ablation to sites of short cycle length activity in the posterior LA (PLA) and observed the termination of arrhythmia in a canine model of AF. Using a sterile pericarditis model, Kumagai et al. (1997, 2000) identified in the septum dominant unstable reentrant circuits of very short CL that maintained AF and could be successfully terminated by focal ablation. Others have reported that in some patients sustained focal activity at the PVs, coronary sinus (CS) or superior vena cava initiated and maintained AF, and could be eliminated by discrete ablation (Jais et al., 1997). However, to this date, whether such sites are either automatic, triggered or reentrant and whether changes in the driver activity would alter spatial frequency gradients, remains unresolved.

The general working hypothesis that acute AF results from activity of a small number of high-frequency reentrant sources localized in one atrium, with fibrillatory conduction to the other atrium is based primarily on results obtained in the isolated, Langendorff-perfused,

sheep heart in the presence of acetylcholine (ACh) (Mandapati et al., 2000). Schuessler et al. (1992) found that with increasing concentrations of ACh, activation patterns characterized by multiple reentrant circuits converted to a single, relatively stable, high-frequency reentrant circuit that resulted in fibrillatory conduction. We localized the sources that maintain AF by a combined use of optical mapping and frequency analysis. Mapping an isolated canine atrial preparation, a systematic evaluation of the effect of ACh on the frequency of rotation in isolated sheep hearts revealed that the DF of the rotors and the AF increase monotonically with [ACh], until attenuated acceleration above 2 μM, with consistent higher DF values in the LA than in the right atrium (RA) (Sarmast et al., 2003).

Our studies on the cholinergic AF in the isolated sheep hearts show the importance of the LA and particularly the PVs as the site with highest DF and source of the arrhythmia maintenance. (Mandapati et al., 2000; Mansour et al., 2001; Jalife et al., 2002) Mandapati et al. (2000) analyzed the DF distribution across the atria in 35 episodes of AF and found that in 66% of all those episodes, 2 sites had the highest DF. Among the 35 AF episodes analyzed, the region surrounding the PV ostium had the highest DF in 80% of AF episodes. Other sites having the highest DF in a particular AF episode decreased in their percentage toward the right atrium free wall (only 4%). Our findings of the PV activity during acute cholinergic AF in the sheep isolated hearts were consistent with the study of Wu et al. (2001) who recorded electrical activity from the atria, the ligament of Marshall and the PVs in the canine model of AF. In that study it was found that the mean cycle length during sustained AF induced in dogs subjected to chronic rapid pacing was shorter in the PVs as compared with those in the left atrial free wall (Wu et al., 2001).

Overall, atrial dilatation and stretch are thought to predispose to AF and dilatation has been found to be an independent risk factor for the development of AF (Vaziri et al., 1994; Psaty et al., 1997; Vasan et al., 1997), but the mechanism is not well understood and is believed to involve mechano-electric feedback (Schotten et al., 2003). We therefore employed yet another sheep model of sustained AF under conditions of acutely increased intra-atrial pressure (IAP) to explore the AF dynamics to test the hypothesis that dilation induces arrhythmogenic sources at the superior PVs during AF (Kalifa et al., 2003). And thus, this article aims at presenting and discussing recent experimental data on wave propagation dynamics and spatio-temporal patterns of activation during stretch-related AF (SRAF) in the atria and in particular in the PLA and the PVs region.

2. Methods and materials

2.1. Isolated hearts

All animal experiments were carried out according to the University of Michigan Committee on Use and Care of Animals and the National Institutes of Health guidelines. Thirteen normal sheep (45–50 kg) were anesthetized with intra-venous bolus injection of propofol (5–10 mg/kg). Hearts were excised with vital organ removal under anesthesia and Langendorff-perfused with warm oxygenated Tyrode's solution (pH 7.4; 95% O_2, 5% CO_2 and 36–38 °C). After perforation of the intra-atrial septum, we sealed all venous orifices except the inferior vena cava for controlling the level of intra-atrial pressure to, unless

otherwise noted, 12 cm H_2O. AF was induced by burst pacing at a cycle length of 10 Hz. AF episodes were sustained for 80.0 ± 15.8 min in this study.

2.2. Optical and electrical mapping

The optical set-up included up to 3 synchronized CCD cameras recording (Fig. 1) from the epicardial right atrial and left atrial appendage (RAA, LAA) and either the endocardial LAA or posterior left atrium (PLA). The latter camera is connected to either a flexible or rigid cardio-endoscope introduced in the left atrium by trans-septal route as described previously (Filgueiras-Rama et al., 2011; Kalifa et al., 2007; Yamazaki et al., 2009). A bolus injection of 15 ml Di-4-ANEPPS (10 mg/mL), enabled recording fluorescence changes from an area of ~3×3 cm^2 (80×80 pixels) for each CCD at 500 frames/s to obtain 5-s movies. To reduce motion artifacts, we added 10 M blebbistatin to the perfusate. Movies of the PLA, LAA and RAA were obtained together with bipolar electrograms of the LAA, left atrium–pulmonary vein (LA-PV) junction, RAA and coronary sinus (CS). The local activation rate of the optical and electrical recordings was determined in the frequency domain as the frequency with maximal power following fast Fourier transform (dominant frequency, DF) (Berenfeld et al., 2011). The maximal DF (DF_{max}) in the optical mapped area was localized and its domain (−0.5 Hz) delineated.

2.3. Analysis of activation patterns and dynamics

Simultaneous endocardial and epicardial movies were analyzed wave-by-wave based on phase domain analysis according to Gray et al. (1998) and performed with the Hilbert transformation (Warren et al., 2003; Yamazaki et al., 2012). Briefly, the instantaneous phase of the action potential recorded at each pixel is determined by transforming the original time-series signals such that every spectral component is shifted by its corresponding quarter cycle. Afterward, the instantaneous phase of the signal is obtained from the inverse tangent of the ratio of the transformed signal to the original signal. The phase angle, with values between $-\pi$ and π radians, is represented as a continuous color scheme to construct a phase map, in which the continuous spatial phase change reflects the process of excitation, repolarization and recovery. Accordingly the upstroke of the waves (wavefront) is detected at the purple–blue (Fig. 2) and blue–green (Figs. 3–5) transitions. For LAA views, representative simultaneous endocardial–epicardial 1-s sample movies for each animal were analyzed during AF. The corresponding phase movie was analyzed with specific attention to wave patterns within the DF_{max} region and patterns of activation were classified as follows. (i) Rotors, defined as a wave rotating around a phase singularity point (Warren et al., 2003; Yamazaki et al., 2012) for more than one rotation; (ii) breakthroughs (BTs): are defined as waves observed at least in part, inside the DF_{max} region, for at least 12 ms (6 frames) and initiated within the field-of-view. In general BTs propagated uniformly centrifugally; however, some BTs propagated preferentially in one direction; (iii) one-way propagation waves were defined as waves emerging from an edge, crossing the entire field, including the DF_{max} region, and lasting at least 12 ms. Following, the epicardial and endocardial patterns were compared and the following 2 groups were formed: (1) Identical endocardial–epicardial wave activation included: endocardial and epicardial reentrant activities that were similar in terms of singularity points location, chirality (wavefront within 90° of each other) and cycle length (± 2 ms). Directionality was classified as identical when besides similar

wave patterns on the epicardium and the endocardium, the endocardial–epicardial wave main directionality was similar. Endocardial and epicardial BTs were classified as simultaneous when they appeared within a 12 ms period. (2) Non-identical endocardial–epicardial wave activation: When epicardial and endocardial patterns were different in terms of patterns and/or wave directionality.

3. Results and discussion

3.1. Intra-atrial pressure and AF

As AF is commonly associated with atrial dilation, (Manyari et al., 1990; Cristal et al., 1976; Murgatroyd and Camm, 1993) we studied an experimental model of sustained AF under conditions of acutely increased intra-atrial pressure to explore AF dynamics. We tested the hypothesis that dilation induces arrhythmogenic sources at the superior PVs during AF. This experimental model was adapted from a well-characterized model of stretch-related AF (Ravelli and Allessie, 1997; Bode et al., 2000; Kalifa et al., 2003) A pressure of 10 cm H_2O was found to be the lower limit to obtain very sustained AF episodes. In comparison, below 10 cm H_2O, AF usually terminates after 10–20 min (Kalifa et al., 2003).

Excitation waves in AF may be highly periodic, both spatially and temporally, having sequential waves propagated with the same spatial pattern and interbeat interval (Skanes et al., 1998). Indeed sequential propagation patterns of STPs may take various forms, including periodic waves emerging from the edge of the recording field, BTs occurring at constant frequencies, and in some cases, stable rotors (Skanes et al., 1998). We found similar STP waves in high SRAF. In Fig. 2 we show an example and quantification of directionality and STP of electrical activation as a function of the IAP during AF. Panel A shows 4 sequential activations in the JPV showing similar waves propagation from the LSPV toward the LA. Clearly, the direction of propagation from LSPV to LAFW was very consistent. In all experiments the directionality of local excitation in the JPV area that corresponded to the highest frequencies correlated strongly with IAP ($r = 0.79$, $P = 0.02$; Fig. 2B). In contrast, the directionality of LAFW to LSPV had a negative and statistically non-significant correlation with pressure ($r = 0.54$, $P = 0.09$). In Fig. 2B, the number of STP wavefronts (normalized to the maximum number of STP wavefronts) in the JPV correlated strongly with IAP ($r = 0.92$, $P = 0.002$).

Similar to the studies presented above, frequency analysis was used to characterize the organization of activity during AF (Berenfeld et al., 2000, 2002) and to establish the likelihood of localizing sources maintaining the AF from which propagation is originating (Mansour et al., 2001). Our study clearly illustrates the strong dependence of frequency of rotors on IAP. Below 10 cm H_2O, the difference between the maximum dominant frequency (DF_{max}) in the JPV and LAFW was not significant (10.8 ± 0.3 versus 10.2 ± 0.3; $P = 0.6$). However, at pressures >10 cm H_2O, DF_{max} in the JPV was significantly higher than that in LAFW (12.0 ± 0.2 and 10.5 ± 0.2 Hz, respectively [mean ± SEM]; $n = 9$; $P < 0.001$). At all pressures, DF_{max} in both JPV and LAFW was significantly higher than the largest frequency recorded in the right atrial free wall (7.8 ± 0.3 Hz; $P < 0.001$). Rotors were observed in the JPV in 3 out 9 experiments and it was found that below 10 cm H_2O, AF terminates because its reentrant sources become slow and unstable. These data are valuable when one considers

that there is evidence that in patients with paroxysmal AF, the diameters of the superior PV ostia are markedly dilated compared with the inferior PV ostia, (Lin et al., 2000) particularly when these PVs are regarded as arrhythmogenic (Yamane et al., 2002). Overall, our data demonstrate that the sources of rapid atrial activation during stretch-related AF are located in the PV region and that their level of spatio-temporal organization correlates with pressure.

3.2. Activation patterns of stretch-related AF

The extent to which spatio-temporal periodic (STP) (Skanes et al., 1998) excitation waves observed in the JPV are generated by either reentrant or ectopic activity in the endocardial and epicardial surfaces of the PV sleeves was further investigated using phase movies generated via Hilbert transformation (see Methods). When characterizing activation patterns, various classes of organized patterns can be identified using phase movies (Fig. 3), including the following: (i) A rotor is identified by the presence of all phases converging onto a singularity point (PS) lasting more than one rotation. (ii) A breakthrough is defined as a wavefront appearing inside the field-of-view and propagating outward in a centrifugal-like pattern. And (iii), spatio-temporally organized periodic (STP) waves are defined as a minimum of four sequential periodic waves emerging from the same location in the field-of-view, with similar direction and inter-wave time interval.

In the atria of 5 normal sheep hearts we identified on average about 1, 6 and 3 wave/s of endo–epi identical reentries, breakthroughs and uniform wave spreading, respectively. In Fig. 3 we demonstrate an alternation between such activation patterns underlying excitation of the PLA during SRAF in our sheep heart model. Each pair of panels in a column is a simultaneous endocardial (top) and epicardial (bottom) snapshot during the AF. Complex AF dynamics at the PLA in this sample normal sheep heart is demonstrated by the sequential phase maps: panels a–f show endo–epi synchronized patterns of excitation on the two surfaces altering from BTs (a) to reentry (b), to collision (c), BTs (d), quasi-plane wave spreading (e) and multiple wavebreaks and reentry (f). This collection of dynamic patterns of activation demonstrates the complexity of tracking AF waves. The intramural dimension of excitation is hidden in our current mapping modalities. More complete information from the intramural patterns of excitation could however assist in better understanding the mechanisms and next we proceed to discuss the possible activation patterns in the thickness of the atrial wall.

3.3. Identical endo–epi activation patterns

We hypothesized that the atrial reentries recorded optically from the surfaces corresponded to 3-dimensional (3-D) scroll waves spanning the thickness of the wall. Therefore, we present the simultaneous epicardial and endoscopy guided endocardial movies in a format enabling the visual reconstruction of the axes or rotation, i.e., the filaments, of the 3-D scroll waves possibly associated with AF (Pertsov and Jalife, 1995). Phase maps of the two recording surfaces of a given atrial area made it possible to detected concurrent epi and endo phase singularities (PSs) around which functional reentry organized. In Fig. 4 we demonstrate two examples of endo–epi activity presented in such a format where the intramural thickness is placed between the endocardial (bottom) and epicardial (top) phase snapshots. In panel A we demonstrate two snapshots of reentrant activity whose pivoting

point is located similarly close to the LPVs both on the endocardial and epicardial surfaces. In this case, it's easy to suggest that the hidden intramural activity adopts the form of a scroll wave whose filament is extended between the two surfaces in what is known as an I-shaped filament (Pertsov, and Jalife, 1995).

Fifteen % of the activations mapped during SRAF in the PLA were found to have identical BT patterns on the endocardial and epicardial surfaces (Yamazaki et al., 2012). In panel B of Fig. 4, an example of such simultaneous breakthrough activity on the epicardial and endocardial surface is shown. In this case, it is easy to conceive that a wave spreading radially outward from a discharge originating from an intramural ectopic focus underlies this surface activation. However, in this case the seemingly obvious suggested ectopic mechanisms may be not so certain after more careful examination: The volume of tissue surrounding the pacemaking cells is likely to exert an electro-tonic load that tends to inhibit the transmembrane potential suprathreshold depolarization needed for the generation of a spreading wave. If the PLA wall at the breakthrough is very thin, then the load may not be fully inhibiting the ectopic-induced wave, however, if the PLA wall is sufficiently thick, then an ectopic pacemaker should be less likely and an intramural scroll wave, whose filament is fully hidden on the mapped surfaces here, may have sufficient room to rotate and spread waves that appear as breakthroughs on the epicardial and endocardial surfaces.

3.4. Non-identical endo–epi activation patterns

As described above, in the normal sheep heart, SRAF was characterized by multiple centrifugal BT activations, wavebreaks and short-lived reentries, all suggesting interplay between reentrant and spontaneous focal discharge mechanisms (Yamazaki et al., 2009). The various patterns could further differ between the endocardial and epicardial surfaces, suggesting the existence of transmural propagation (Everett et al., 2010) and linked to increased stability of AF (Eckstein et al., 2011). In Fig. 5 we present and discuss data on such transmural dissociated excitation patterns. On the left side of panel A, the epicardial phase snapshot shows reentrant activity, and the simultaneous endocardial snapshot shows a breakthrough pattern. On the right side we present the same snapshots in a format that illustrates a possible scroll wave with a bent filament, also known as L-shaped filament, which may underlie such non-identical surfaces' activation patterns. Accordingly, one free-end of the filament resides in the epicardial surface while the other free-end of the filament is extending toward the outside of the fields mapped. It should be noted that the latter free-end of the filament must be at a myocardial boundary somewhere, and based on a topological theorem it cannot reside inside the tissue, even not at the boundary of a scar 3-D island (Pertsov et al., 2000). The possibility of a focal discharge in this case is not conceivable. This example also highlights the importance of simultaneous dual surfaces mapping. In case only the breakthrough activity would have been mapped on a single surface, this would erroneously suggest that the origin of this AF wave is an ectopic discharge. In panel B of Fig. 5 we discuss yet another example of dissociated activity. On the left panel two counter-rotating reentries are seen on the epicardial surface and two simultaneous breakthroughs are seen on the endocardial surface. On the right panel we show the combined phase snapshots with a hypothesized U-shaped filament connecting the two singularity points on the same surface. It is of course possible that the two reentries do not

belong to the same scroll wave and are actually two separated L-shaped filaments as in panel A. This panel again highlights the importance of dual surface mapping to better characterize the patterns of excitation in relation to the possible ectopic or reentrant activity.

3.5. Breakthroughs and scroll waves in the PV region

Overall, in our study of SRAF in the sheep isolated hearts we found 59% of the waves mapped in the PLA to be identical and 41% of the waves to be different (dissociated) between the endo–epicardial surfaces. Comparing the lifespan of endo–epicardial identical reentries (that is, I-filament scroll waves) in term of the number of rotations we found that while in normal hearts I-filament scroll waves never lasted more than 3 rotations, we found examples of I-filament scroll waves lasting 6 rotations or more in 12/16 movies from another model of persistent AF sheep hearts (Yamazaki et al., 2012). In a subset of 47 AF waves from the LAA of 5 normal animals the average number of simultaneous endocardial and epicardial BTs was significantly larger than rotors (3.8 ± 1.6/s versus 1.0 ± 1.4/s, respectively) (Yamazaki et al., 2012). In a previous study of AF in sheep hearts we found that the BTs during AF were the most common pattern of activation and they tended to cluster at the middle of the PLA, where the radius encircling about 75% of the BTs in 6 hearts resided in the area between the PVs, and not including the PVs themselves (Tanaka et al., 2007). Here, in SRAF in 4 other normal sheep hearts, there was neither preference in spatial distribution of the density of the breakthroughs at any of either the left or right PVs, nor to any other non-PV region in the PLA (see Fig. 6). In yet 4 other normal sheep hearts during SRAF multiple rotor PSs formed at the PLA during each 1 s episode of AF. The rotors PS points were traced for the duration of the rotor and their location has been superimposed on the corresponding PLA background anatomical pictures of each of the 4 hearts. Panels b, c and f of Fig. 3 show examples of those PSs and demonstrates that they are confined to the PLA with some small meandering and drifting mostly in the vicinity of the ostia and antral aspects of any of the PVs.

4. Conclusions

There is experimental evidence that increasing stretch increases the dominance of the PVs during AF in isolated hearts (Mandapati et al., 2000; Kalifa et al., 2003) and ectopic activity in the isolated PVs, (Chang et al., 2007) but the ionic mechanisms underlying such effect are not clear and the ability of the PVs to favorably host functional reentry during stretch cannot be excluded (Mandapati et al., 2000; Kalifa et al., 2003). In single cardiomyocytes isolated from the PVs of rabbits Seol et al., (2008) recently found stretch-induced anionic and cationic currents however it is not clear whether the dominance of the PVs in the initiation and maintenance of AF depends on spatial heterogeneity in the distribution of those currents, or alternatively in the relative increase in stretch due to the relative thinner myocardial wall in the PV sleeve compared with the walls of the atria (Nathan and Eliakim, 1966; Seol et al., 2008). We used a combination of optical mapping and spectral analysis to study SRAF in normal isolated sheep hearts and we have found rapid sources that are located in the PLA and PV region and their activation frequency and level of organization correlates with intra-atrial pressure. Analysis of the surfaces' optical mapping data in the phase domain reveals that activation of the PLA consisted of alternating patterns of

breakthroughs, reentries and relatively simple waves swiping through the field-of-view. The patterns on the endocardial and epicardial PLA surface at any given moment of time of the SRAF could be either identical or not identical, and the activity in the 3-D thickness of the PLA wall is hypothesized to conform to either ectopic discharge or scroll waves. However, clear evidence for the presence of such mechanisms is lacking and will require further investigation.

Acknowledgments

References

Benussi S, et al. A simple way to treat chronic atrial fibrillation during mitral valve surgery: the epicardial radiofrequency approach. Eur J Cardiothorac Surg. 2000; 17:524–529. [PubMed: 10814914]

Berenfeld O, et al. Time- and frequency-domain analyses of atrial fibrillation activation rate: the optical mapping reference. Heart Rhythm. 2011; 8:1758–1765. [PubMed: 21699849]

Berenfeld O, et al. Spatially distributed dominant excitation frequencies reveal hidden organization in atrial fibrillation in the Langendorff-perfused sheep heart. J Cardiovasc Electrophysiol. 2000; 11:869–879. [PubMed: 10969749]

Berenfeld O, et al. Frequency-dependent breakdown of wave propagation into fibrillatory conduction across the pectinate muscle network in the isolated sheep right atrium. Circ Res. 2002; 90:1173–1180. [PubMed: 12065320]

Bode F, et al. Gadolinium decreases stretch-induced vulnerability to atrial fibrillation. Circulation. 2000; 101:2200–2205. [PubMed: 10801762]

Brunton TL, Fayrer J. Note on independent pulsation of the pulmonary veins and vena cava. Proc Roy Soc Lond. 1876; 25:174–176.

Cha TJ, et al. Atrial tachycardia remodeling of pulmonary vein cardiomyocytes: comparison with left atrium and potential relation to arrhythmogenesis. Circulation. 2005; 111:728–735. [PubMed: 15699259]

Chang SL, et al. Mechanoelectrical feedback regulates the arrhythmogenic activity of pulmonary veins. Heart. 2007; 93:82–88. [PubMed: 16905626]

Chen J, et al. Dynamics of wavelets and their role in atrial fibrillation in the isolated sheep heart. Cardiovasc Res. 2000; 48:220–232. [PubMed: 11054469]

Chen LY, Shen WK. Epidemiology of atrial fibrillation: a current perspective. Heart Rhythm. 2007; 4:S1–S6. [PubMed: 17336876]

Chen YC, et al. Effects of thyroid hormone on the arrhythmogenic activity of pulmonary vein cardiomyocytes. J Am Coll Cardiol. 2002; 39:366–372. [PubMed: 11788233]

Chen YJ, et al. Arrhythmogenic activity of cardiac muscle in pulmonary veins of the dog: implication for the genesis of atrial fibrillation. Cardiovasc Res. 2000; 48:265–273. [PubMed: 11054473]

Chen YJ, et al. Effects of rapid atrial pacing on the arrhythmogenic activity of single cardiomyocytes from pulmonary veins – implication in initiation of atrial fibrillation. Circulation. 2001; 104:2849–2854. [PubMed: 11733406]

Cheung DW. Electrical activity of the pulmonary vein and its interaction with the right atrium in the guinea-pig. J Physiol. 1981a; 314:445–456. [PubMed: 7310698]

Cheung DW. Pulmonary vein as an ectopic focus in digitalis-induced arrhythmia. Nature. 1981b; 294:582–584. [PubMed: 7312048]

Cristal N, et al. Atrial fibrillation developing in the acute phase of myocardial infarction. Prognostic implications. Chest. 1976; 70:8–11. [PubMed: 1277939]

de Bakker JMT, et al. Basic and clinical electrophysiology of pulmonary vein ectopy. Cardiovasc Res. 2002; 54:287–294. [PubMed: 12062334]

Eckstein J, et al. Time course and mechanisms of endo-epicardial electrical dissociation during atrial fibrillation in the goat. Cardiovasc Res. 2011; 89:816–824. [PubMed: 20978006]

Ehrlich JR, et al. Cellular electrophysiology of canine pulmonary vein cardiomyocytes: action potential and ionic current properties. J Physiol. 2003; 551:801–813. [PubMed: 12847206]

Everett TH, et al. Transmural characteristics of atrial fibrillation in canine models of structural and electrical atrial remodeling assessed by simultaneous epicardial and endocardial mapping. Heart Rhythm. 2010; 7:506–517. [PubMed: 20184976]

Filgueiras-Rama D, et al. High-resolution endocardial and epicardial optical mapping in a sheep model of stretch-induced atrial fibrillation. J Vis Exp. 2011

Gray RA, et al. Spatial and temporal organization during cardiac fibrillation. Nature. 1998; 392:75–78. [PubMed: 9510249]

Haissaguerre M, et al. Catheter ablation of chronic atrial fibrillation targeting the reinitiating triggers. J Cardiovasc Electrophysiol. 2000a; 11:2–10. [PubMed: 10695453]

Haissaguerre M, et al. Spontaneous initiation of atrial fibrillation by ectopic beats originating in the pulmonary veins. N Engl J Med. 1998; 339:659–666. [PubMed: 9725923]

Haissaguerre M, et al. Mapping-guided ablation of pulmonary veins to cure atrial fibrillation. Am J Cardiol. 2000b; 86:9K–19K.

Hocini M, et al. Electrical conduction in canine pulmonary veins – electrophysiological and anatomic correlation. Circulation. 2002; 105:2442–2448. [PubMed: 12021234]

Honjo H, et al. Pacing-induced spontaneous activity in myocardial sleeves of pulmonary veins after treatment with ryanodine. Circulation. 2003; 107:1937–1943. [PubMed: 12668519]

Jais P, et al. A focal source of atrial fibrillation treated by discrete radiofrequency ablation. Circulation. 1997; 95:572–576. [PubMed: 9024141]

Jalife J, et al. Mother rotors and fibrillatory conduction: a mechanism of atrial fibrillation. Cardiovasc Res. 2002; 54:204–216. [PubMed: 12062327]

Kalifa J, et al. Intra-atrial pressure increases rate and organization of waves emanating from the superior pulmonary veins during atrial fibrillation. Circulation. 2003; 108:668–671. [PubMed: 12900337]

Kalifa J, et al. Endoscopic fluorescence mapping of the left atrium: a novel experimental approach for high resolution endocardial mapping in the intact heart. Heart Rhythm. 2007; 4:916–924. [PubMed: 17599678]

Knight BP, et al. Cost comparison of radiofrequency modification and ablation of the atrioventricular junction in patients with chronic atrial fibrillation. Circulation. 1997; 96:1532–1536. [PubMed: 9315543]

Kumagai K, et al. Simultaneous multisite mapping studies during induced atrial fibrillation in the sterile pericarditis model. Insights into the mechanisms of its maintenance. Circulation. 1997; 95:511–521. [PubMed: 9008471]

Kumagai K, et al. Single site radiofrequency catheter ablation of atrial fibrillation: studies guided by simultaneous multisite mapping in the canine sterile pericarditis model. J Am Coll Cardiol. 2000; 36:917–923. [PubMed: 10987620]

Lewis, T. The Mechanism and Graphic Registration of the Heart Beat. Shaw & Sons; London: 1925. p. 319-374.

Lin WS, et al. Pulmonary vein morphology in patients with paroxysmal atrial fibrillation initiated by ectopic beats originating from the pulmonary veins: implications for catheter ablation. Circulation. 2000; 101:1274–1281. [PubMed: 10725287]

Mandapati R, et al. Stable microreentrant sources as a mechanism of atrial fibrillation in the isolated sheep heart. Circulation. 2000; 101:194–199. [PubMed: 10637208]

Mansour M, et al. Left-to-right gradient of atrial frequencies during acute atrial fibrillation in the isolated sheep heart. Circulation. 2001; 103:2631–2636. [PubMed: 11382735]

Manyari DE, et al. Atrial and ventricular arrhythmias in asymptomatic active elderly subjects: correlation with left atrial size and left ventricular mass. Am Heart J. 1990; 119:1069–1076. [PubMed: 2330865]

Melnyk P, et al. Comparison of ion channel distribution and expression in cardiomyocytes of canine pulmonary veins versus left atrium. Cardiovasc Res. 2005; 65:104–116. [PubMed: 15621038]

Miyauchi Y, et al. Heterogeneous pulmonary vein myocardial cell repolarization implications for reentry and triggered activity. Heart Rhythm. 2005; 2:1339–1345. [PubMed: 16360087]

Moe GK, Abildskov JA. Atrial fibrillation as a self-sustaining arrhythmia independent of focal discharges. Am Heart J. 1959; 58:59–70. [PubMed: 13661062]

Morillo CA, et al. Chronic rapid atrial pacing: structural, functional, and electrophysiological characteristics of a new model of sustained atrial fibrillation. Circulation. 1995; 91:1588–1595. [PubMed: 7867201]

Murgatroyd FD, Camm AJ. Atrial arrhythmias. Lancet. 1993; 341:1317–1322. [PubMed: 7684105]

Nathan H, Eliakim M. The junction between the left atrium and the pulmonary veins. An anatomic study of human hearts. Circulation. 1966; 34:412–422. [PubMed: 5922708]

Nattel S. Pulmonary vein cellular electrophysiology and atrial fibrillation: does basic research help us understand clinical pulmonary-vein arrhythmogenesis? Heart Rhythm. 2005; 2:1346. [PubMed: 16360088]

Oral H, et al. Circumferential pulmonary-vein ablation for chronic atrial fibrillation. N Engl J Med. 2006; 354:934–941. [PubMed: 16510747]

Patterson E, et al. Sodium-calcium exchange initiated by the Ca^{2+} transient: an arrhythmia trigger within pulmonary veins. J Am Coll Cardiol. 2006; 47:1196–1206. [PubMed: 16545652]

Patterson E, et al. Triggered firing in pulmonary veins initiated by in vitro autonomic nerve stimulation. Heart Rhythm. 2005; 2:624–631. [PubMed: 15922271]

Pertsov, AM.; Jalife, J. Three-dimensional Vortex-like reentry. In: Zipes, DP.; Jalife, J., editors. Cardiac Electrophysiology from Cell to Bedside. W.B. Saunders Company; Philadelphia: 1995. p. 403-410.

Pertsov AM, et al. Topological constraint on scroll wave pinning. Phys Rev Lett. 2000; 84:2738–2741. [PubMed: 11017313]

Psaty BM, et al. Incidence of and risk factors for atrial fibrillation in older adults. Circulation. 1997; 96:2455–2461. [PubMed: 9337224]

Quinn TA, Kohl P. Mechano-sensitivity of cardiac pacemaker function: pathophysiological relevance, experimental implications, and conceptual Integration with other mechanisms of rhythmicity. Prog Biophys Mol Biol. 2012; 110 (2–3):257–268. [PubMed: 23046620]

Ravelli F, Allessie M. Effects of atrial dilatation on refractory period and vulnerability to atrial fibrillation in the isolated Langendorff-perfused rabbit heart. Circulation. 1997; 96:1686–1695. [PubMed: 9315565]

Sanders P, et al. Spectral analysis identifies sites of high-frequency activity maintaining atrial fibrillation in humans. Circulation. 2005; 112:789–797. [PubMed: 16061740]

Sarmast F, et al. Cholinergic atrial fibrillation: I-K, I-ACh gradients determine unequal left/right atrial frequencies and rotor dynamics. Cardiovasc Res. 2003; 59:863–873. [PubMed: 14553826]

Scherf D. Studies on auricular tachycardia caused by aconitine administration. Proc Soc Exp Biol Med. 1947; 64:233–239. [PubMed: 20287386]

Schotten U, et al. The role of atrial dilatation in the domestication of atrial fibrillation. Prog Biophys Mol Biol. 2003; 82:151–162. [PubMed: 12732275]

Schuessler RB, et al. Cholinergically mediated tachyarrhythmias induced by a single extrastimulus in the isolated canine right atrium. Circ Res. 1992; 71:1254–1267. [PubMed: 1394883]

Seol CA, et al. Stretch-activated currents in cardiomyocytes isolated from rabbit pulmonary veins. Prog Biophys Mol Biol. 2008; 97:217–231. [PubMed: 18353429]

Skanes AC, et al. Spatiotemporal periodicity during atrial fibrillation in the isolated sheep heart. Circulation. 1998; 98:1236–1248. [PubMed: 9743516]

Tanaka K, et al. Spatial distribution of fibrosis governs fibrillation wave dynamics in the posterior left atrium during heart failure. Circ Res. 2007; 101:839–847. [PubMed: 17704207]

Vasan RS, et al. Distribution and categorization of echocardiographic measurements in relation to reference limits: the Framingham Heart Study: formulation of a height- and sex-specific classification and its prospective validation. Circulation. 1997; 96:1863–1873. [PubMed: 9323074]

Vaziri SM, et al. The Framingham Heart Study. Echocardiographic predictors of nonrheumatic atrial fibrillation. Circulation. 1994; 89:724–730. [PubMed: 8313561]

Warren M, et al. Blockade of the inward rectifying potassium current terminates ventricular fibrillation in the guinea pig heart. J Cardiovasc Electrophysiol. 2003; 14:621–631. [PubMed: 12875424]

Werdich AA, Brzezinski A, Jeyaraj D, Sabeh MK, Ficker E, Wan X, MacRae CA, Rosenbaum DS. The zebrafish as a novel animal model to study the molecular mechanisms of mechano-electrical feedback in the heart. Prog Biophys Mol Biol. 2012; 110 (2–3):154–165. [PubMed: 22835662]

Wu TJ, et al. Pulmonary veins and ligament of Marshall as sources of rapid activations in a canine model of sustained atrial fibrillation. Circulation. 2001; 103:1157–1163. [PubMed: 11222481]

Yamane T, et al. Dilatation as a marker of pulmonary veins initiating atrial fibrillation. J Interv Card Electrophysiol. 2002; 6:245–249. [PubMed: 12154327]

Yamazaki M, et al. Heterogeneous atrial wall thickness and stretch promote scroll waves anchoring during atrial fibrillation. Cardiovasc Res. 2012; 94:48–57. [PubMed: 22227155]

Yamazaki M, et al. Mechanisms of stretch-induced atrial fibrillation in the presence and the absence of adrenocholinergic stimulation: interplay between rotors and focal discharges. Heart Rhythm. 2009; 6:1009–1017. [PubMed: 19560089]
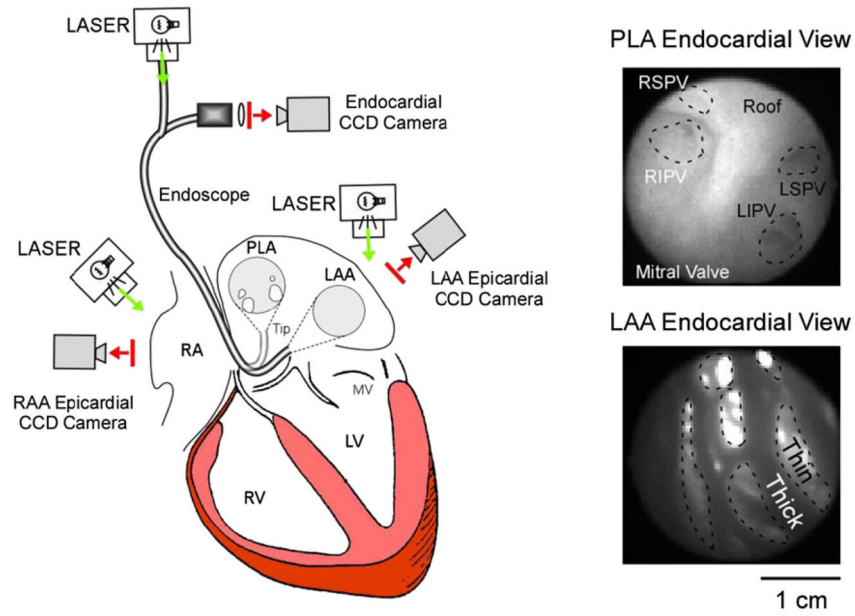
Fig. 1.
Schematic diagram of the experimental optical mapping setting. Up to 3-CCDs were used for simultaneous mapping of the electrical excitation patterns on the epicardium and endocardium of the atria. The endoscope used was of the flexible or the rigid (not shown) type. The panels on the right are endocardial views of the anatomy of the posterior LA wall (PLA, top) and the LA appendage and free wall (LAA, bottom). (Reproduced from Yamazaki et al., 2012).
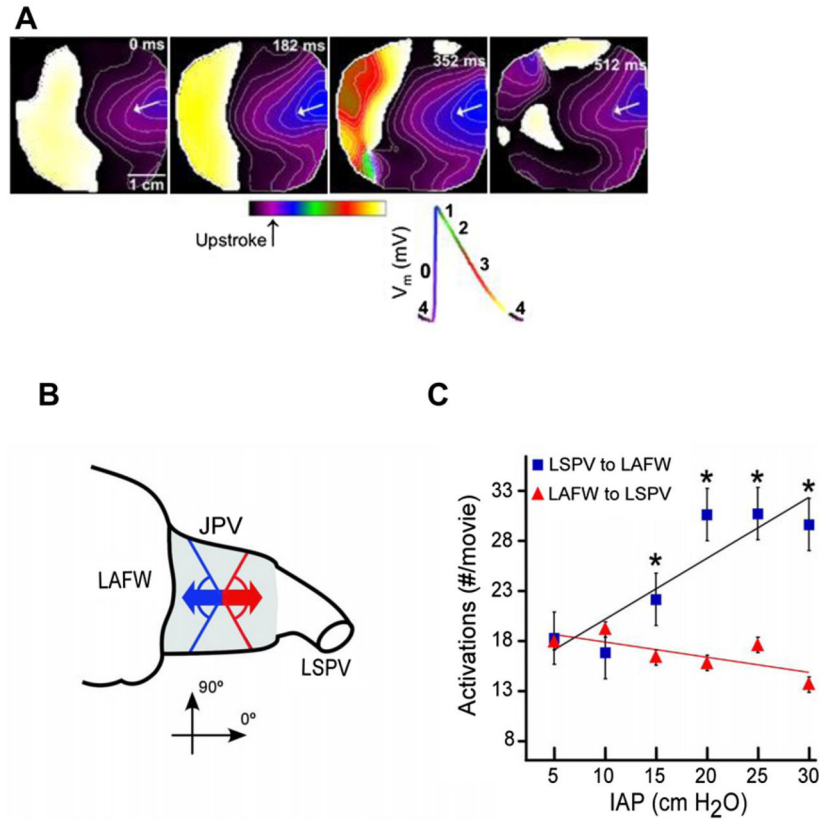
Fig. 2.
Patterns of activation in the atria-PV junction during SRAF. A) Four spatio-temporally organized periodic waves (At 0, 182, 352 and 512 ms, respectively) coming from the PLA region toward the LAA. Isochrones are plotted at 10 ms intervals. Bottom, key for the different phases of the action potential is color-coded (Reproduced from Filgueiras-Rama et al. 2011). B) Schematic directionality of activity from the PVs to LAFW (blue arrow) and from the LAFW to LSPV (red arrow) assessed at the junctional PV (JPV) region (shaded area). C) Number of activations (mean ± SEM) moving from left superior PV (LSPV) to LA free wall (LAFW) and from LAFW to LSPV (*$P < 0.01$ compared with LAFW to LSPV). Colors are the same as in B. (Reproduced from Kalifa et al., 2003).
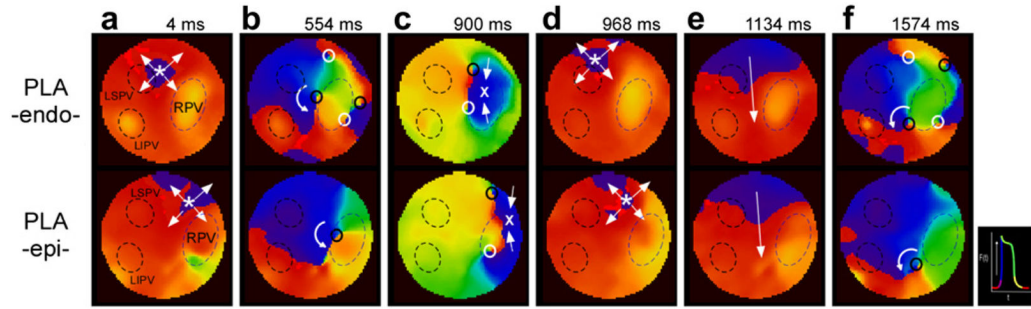
Fig. 3.
Complex AF dynamics at the PLA of normal sheep hearts. Sequential phase maps obtained simultaneously from PLA-endo (top row) and PLA-epi (bottom row) during AF in a sample heart. Panels a–f show synchronized patterns of excitation on the two surfaces altering from breakthroughs (a) to reentry (b), to collision (c), breakthroughs (d), coasting (e) and multiple wavebreaks and reentry (f). LSPV; left superior PV, LIPV; left inferior pulmonary vein, RPV; right PV.
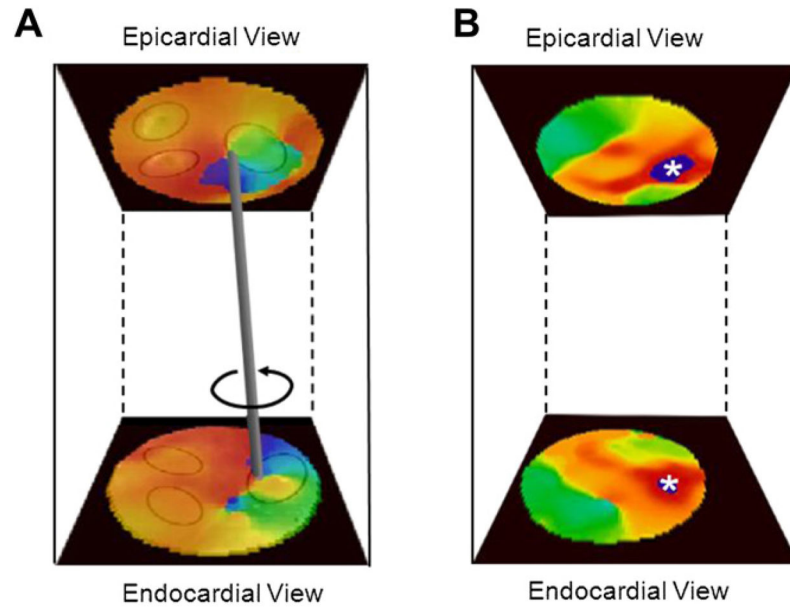
Fig. 4.
Examples of simultaneous and identical activation pattern on the endocardium and epicardium of the PLA of a sheep heart during SRAF. A) A representative phase snapshots from endocardial and epicardial surfaces showing synchronous rotational activity with pivoting point near the RPV. B) Synchronous breakthrough activity on the two opposing surfaces.
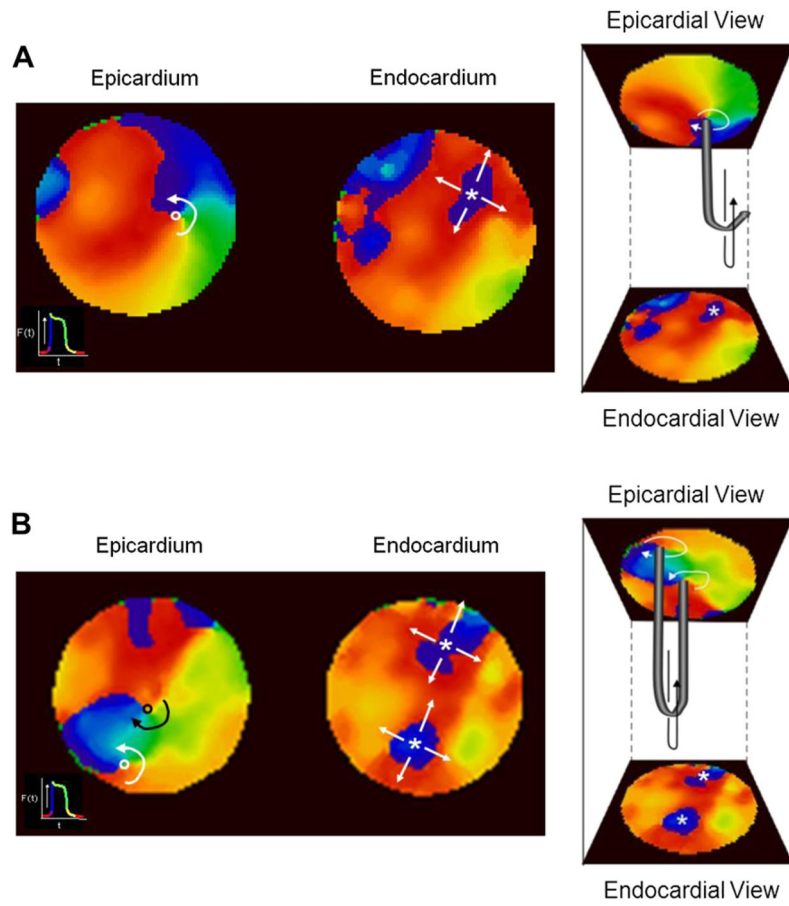
Fig. 5.
Examples of endocardial–epicardial reentrant-breakthrough dissociated activation patterns suggesting either an L-shaped filament (A) or a U-shaped filament (B) of scroll waves.
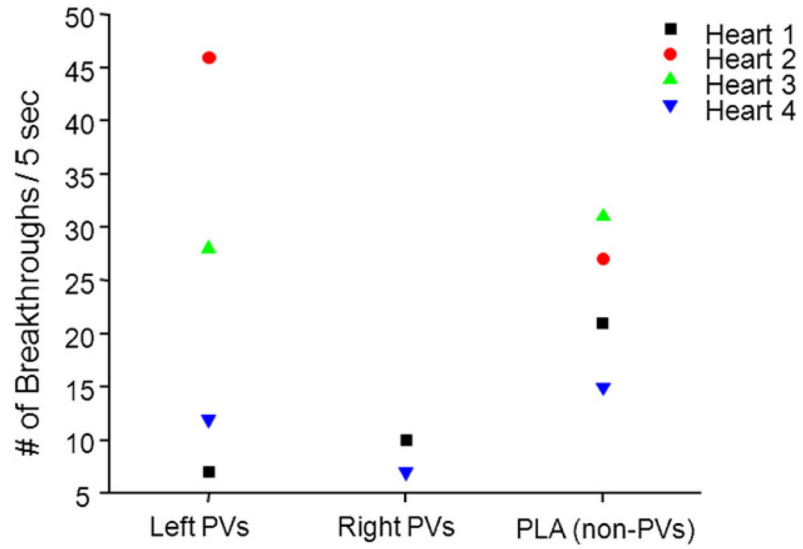
Fig. 6.
Spatial distribution of breakthrough activity in the PLA during SRAF in 4 sample isolated sheep hearts. The number of breakthroughs varies mostly in the left PVs (between 6 to 46 breakthroughs per 5 sec activity) but there is no preferential breakthrough site within the PLA. PLA; posterior LA.